

Electron transfer in ionic fluorine compounds following multiple ionization by 22-MeV carbon ions

O. Benka, R. L. Watson, K. Parthasaradhi, J. M. Sanders, and R. J. Maurer

Cyclotron Institute and Department of Chemistry, Texas A&M University, College Station, Texas 77843

(Received 21 June 1982)

The spectra of K x rays emitted by thin targets of the alkali-metal and alkaline-earth fluorides under bombardment with 22-MeV carbon ions were measured with a curved crystal spectrometer. Comparison of the satellite intensity distributions with that obtained for neon under similar conditions revealed that electron transfer within the K -hole lifetime ($\sim 10^{-13}$ sec) is highly probable even for these highly ionic compounds. A detailed analysis of the satellite intensity distribution obtained for LiF yielded a rate constant for KL^1 - KL^0 transfer equal to 30% that for K -vacancy decay. The spectra for KF, SrF₂, and BaF₂ show evidence of resonant electron transfer (RET) associated with the matching of the $2p$ binding energies of fluorine atoms in KL^1 states with the outer np binding energies of adjacent metal ions, in agreement with previous findings. Also, an anomalously low KL^2 intensity, indicative of RET in association with this double L -hole state, was observed for CaF₂. An additional component contributing to the enhancement of the KL^0 peak was attributed to secondary-electron ionization.

I. INTRODUCTION

Investigations of the effects of chemical environment on the relative intensities of $K\alpha$ x-ray satellites produced by heavy-ion bombardment have demonstrated the importance of L -vacancy filling processes occurring within the K -hole lifetime. Most measurements to date have been performed on elements having $Z > 10$, for which the L shell is inside the valence shell. The probability of electron transfer to the L shell following K -plus-multiple- L -shell ionization in Al, S, and Cl has been found to be of the order of 5%.^{1,2}

Recently, such studies have been extended to fluorine, where the effects are expected to be more pronounced because in this case the valence shell is the L shell. Uda *et al.*³ have found L -vacancy filling probabilities as high as 50% in covalent fluorine compounds, such as Teflon. In addition, the measurements of Benka *et al.*⁴ on alkali-metal and alkaline-earth fluorides have shown that a resonant transfer of electrons from neighboring atoms can occur when level-matching conditions exist.

Until now, all of the reported measurements on fluorine compounds have been carried out using thick targets. With thick targets, only the KL^0 , KL^1 , and KL^2 satellite groups, arising from initial states having one K vacancy and 0, 1, and 2 L vacancies, respectively, are observable because the rest of the x-ray groups lie above the K -absorption edge of fluorine. In the present work, the higher satellite

groups are examined using 22-MeV carbon ions incident on thin targets having minimal self-absorption. By comparing the intensity distributions of the fluorine satellite groups with the satellite intensity distribution obtained for neon (using a closed gas cell), rates for refilling fluorine L -shell vacancies were determined. Additional evidence for resonant electron transfer associated with the matching of $2p$ binding energies of fluorine ions with the outer np binding energies of adjacent metal ions was found, and a mechanism contributing to the enhancement of the KL^0 peak intensity was identified to be secondary-electron ionization.

II. EXPERIMENTAL METHODS

The experiments were performed using a beam of 22-MeV C^{3+} ions provided by the Texas A&M University variable-energy cyclotron. This beam was selected because it was found to produce relatively high intensities of all the $K\alpha$ satellite groups of fluorine from KL^0 to KL^7 . Additionally, transitions from high Rydberg states to the K shell in carbon lie below the energies of the fluorine KL^0 line and hence do not interfere with any of the lines of interest.

Thin targets of LiF, NaF, KF, RbF, MgF₂, CaF₂, SrF₂, and BaF₂ were made by vacuum evaporation onto 20- $\mu\text{g}/\text{cm}^2$ carbon backing foils. The thickness of the target material was 10 $\mu\text{g}/\text{cm}^2$ or less as deduced from the fact that no evidence of absorption discontinuities caused by the K -absorption edge

could be seen in any of the spectra. Since only the relative intensities were of interest, it was not necessary to know the target thicknesses accurately.

As a check on the possibility that the compounds undergo decomposition during vacuum evaporation, spectra were also taken of thick targets consisting of pressed pellets of the powdered compounds. It was found that the relative intensities of the KL^0 , KL^1 , and KL^2 x-ray groups for both thin and thick targets were in good agreement. Such a comparison is shown in Fig. 1 for NaF.

The spectral measurements were performed with a 12.7-cm curved crystal spectrometer employing a flow proportional counter (P-10 gas at 1 atm). The proportional counter window consisted of $65\text{-}\mu\text{g}/\text{cm}^2$ stretched polypropylene, and the spectrometer diffraction crystal was rubidium acid phthalate (RAP). X rays emitted from the target were observed at 90° to the beam direction by the spectrometer, which was mounted with the plane of its focal circle normal to the beam direction. In order to minimize self-absorption by the target and yet achieve a reasonably large thickness with respect to the ion beam, the target was oriented such that its surface normal was at a 45° angle with respect to both the horizontal and vertical planes defined by the beam axis.

As mentioned above, the Ne spectrum was measured using a closed gas cell. The beam-entrance

window was constructed from a $1.9\text{-mg}/\text{cm}^2$ Havar foil and the x-ray window (located on the side of the gas cell at 90° to the beam and 1 cm from the beam-entrance window) consisted of $65\text{-}\mu\text{g}/\text{cm}^2$ stretched polypropylene. A gas pressure of approximately 30 mbar provided sufficient x-ray intensity and caused little self-absorption over the 2.5-mm path length from the beam axis to the x-ray window. Because of the relatively high pressure used, the charge-state distribution of the carbon ions was assumed to be equilibrated, with the average charge state being essentially the same as that for the solid fluorine compound measurements ($\bar{q} \approx 5.1$). Additional details concerning the Ne measurements will be given elsewhere.⁵

III. RESULTS

Spectra obtained for the alkali-metal and alkaline-earth fluorides are compared in Fig. 2. The x-ray groups KL^0 to KL^5 appear in these spectra in order of increasing energy. It is evident that rather large relative intensity differences occur for the first few satellite groups (KL^0 to KL^3) among the various compounds, while the relative intensities of the higher satellite groups are rather similar. As one goes down a series (LiF—RbF, and MgF_2 — BaF_2), it is seen that the KL^0 relative intensity increases

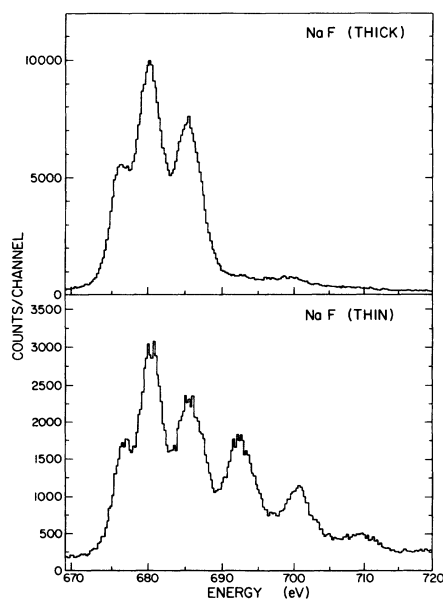


FIG. 1. Comparison of fluorine $K\alpha$ satellite spectra excited by 22-MeV carbon ions incident on a thick NaF target (top) and a thin NaF target (bottom). Satellites beyond KL^2 in the thick-target spectrum are obscured by the fluorine K -absorption edge.

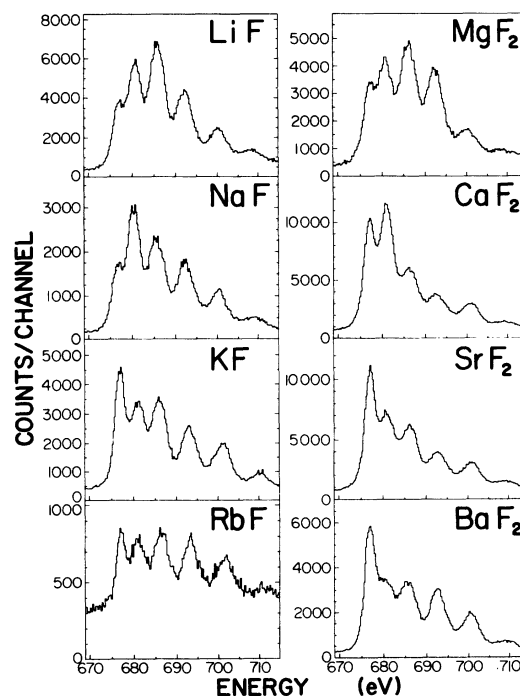


FIG. 2. Fluorine $K\alpha$ satellite spectra excited by 22-MeV carbon ions incident on thin targets of alkali-metal and alkaline-earth fluorides.

dramatically.

The intensities of the individual satellite groups were extracted by means of a least-squares-fitting program (FACELIFT). Each satellite group was represented by a Voigt function having a variable Gaussian width and a fixed Lorentzian width of 0.3 eV. In the cases of LiF and MgF₂, the KL⁰ peak was found to be somewhat asymmetric. Therefore it was necessary to represent the KL⁰ peak by two Voigt components in these two instances. Photoelectron spectroscopic measurements have shown that the fluorine 2*p* band structure in these compounds is asymmetric with a width of about 3 eV.⁶

Table I lists the relative intensities of the Kα satellite groups for all the compounds studied, as obtained directly from the fitting procedure (i.e., they are uncorrected for absorption, efficiency, and fluorescence yield). Repetitive measurements indicated that the uncertainties in these relative intensities are of the order of 15% or less. Estimates of the corrections for crystal reflectivity, for absorption in the proportional-counter window and target self-absorption, and for proportional-counter efficiency (≈5%) were much smaller than the experimental reproducibility, and hence were neglected.

A convenient parameter for characterizing the Kα satellite relative intensity distribution is the apparent average *L*-vacancy fraction *p_L* computed from the satellite relative intensities *N*(*n*) according to the relationship

$$p_L = \frac{\bar{n}}{8} = \frac{1}{8} \sum_{n=1}^7 nN(n),$$

where *n* is the number of *L*-shell vacancies. As is shown in Fig. 3, the relative intensity distributions for LiF, NaF, and MgF₂ are closely represented by binomial distributions having binomial probabilities equal to the *p_L* values calculated for these spectra (0.267, 0.259, and 0.256, respectively). The *L*-vacancy distribution determined for Ne was also well represented by a binomial distribution having *p_L* = 0.32. Since Ne is a monatomic gas whose

outermost shell is the *L* shell, filling of *L* vacancies can only occur as a result of collisions between primary collision-produced recoil ions and surrounding neutral Ne atoms. Mann *et al.*⁷ have shown that typical Ne-ion recoil velocities for heavy-ion projectiles are ≤ 10⁶ cm/sec. Thus, at the pressure used in the Ne measurements (20 Torr), the mean time between collisions is greater than 10⁻¹⁰ sec. This is much longer than the mean lifetimes of all the satellite and hypersatellite transitions except the satellite transitions arising from the metastable ³P,³S(KL⁵), ⁴P(KL⁶), and ³P(KL⁷) states. It is to be expected, therefore, that the x-ray relative intensities in the Ne spectrum after correction for fluorescence yield and overlap of metastable transitions, should provide an accurate representation of the primary vacancy distribution. The fact that the *p_L* values for LiF, NaF, and MgF₂ are considerably smaller than the *p_L* value for the *L*-vacancy distribution of Ne therefore indicates that interatomic electron transfer is highly probable even in these very ionic compounds. A visual illustration of the effect of *L*-vacancy filling on a satellite intensity distribution is given in Fig. 4 where the NaF x-ray intensities, corrected for fluorescence yield but not for *L*-vacancy transfer, are compared with the primary *L*-vacancy distribution determined from the Ne spectrum.

IV. ANALYSIS AND DISCUSSION

A. *L*-vacancy refilling rates

The overlapping contributions of the numerous possible multiplet components in the Kα satellite spectra greatly complicate the extraction of quantitative information concerning electron transfer. Consider, for example, the decay channels for a single KL^{*n*} multiplet state *j*; the *K* hole may decay by x-ray emission with rate constant λ_x(*n*,*j*), or by Auger emission with rate constant λ_A(*n*,*j*), or the *L* hole may be filled by electron transfer with rate constant λ_t(*n*,*j*). The probability of decay by process *i* (where *i* may be x, A, or t) is given by

TABLE I. Experimental fluorine Kα x-ray satellite group relative intensities for the alkali-metal and alkaline-earth fluorides.

Compound	KL ⁰	KL ¹	KL ²	KL ³	KL ⁴	KL ⁵
LiF	0.104	0.232	0.294	0.211	0.107	0.051
NaF	0.133	0.237	0.264	0.202	0.118	0.046
KF	0.214	0.199	0.233	0.175	0.138	0.047
RbF	0.138	0.189	0.234	0.209	0.172	0.058
MgF ₂	0.125	0.223	0.302	0.214	0.102	0.034
CaF ₂	0.249	0.291	0.202	0.132	0.092	0.034
SrF ₂	0.278	0.220	0.225	0.146	0.102	0.029
BaF ₂	0.251	0.166	0.230	0.190	0.125	0.039

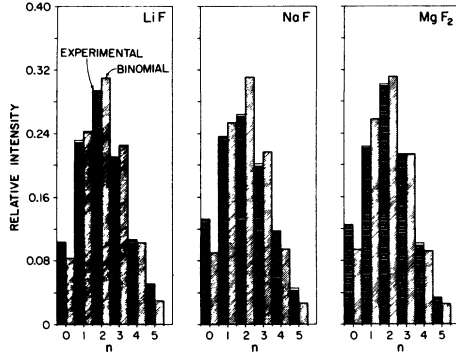


FIG. 3. Comparison of the satellite relative intensities for LiF, NaF, and MgF₂ with binomial distributions.

$$f_i(n,j) = \frac{\lambda_i(n,j)}{\lambda_T(n,j)}, \quad (1)$$

where

$$\begin{aligned} \lambda_T(n,j) &= \lambda_x(n,j) + \lambda_A(n,j) + \lambda_t(n,j) \\ &= \lambda_K(n,j) + \lambda_t(n,j). \end{aligned}$$

The probability for K-hole decay is then

$$\begin{aligned} f_K(n,j) &= f_x(n,j) + f_A(n,j) \\ &= \frac{\lambda_x(n,j) + \lambda_A(n,j)}{\lambda_T(n,j)}. \end{aligned}$$

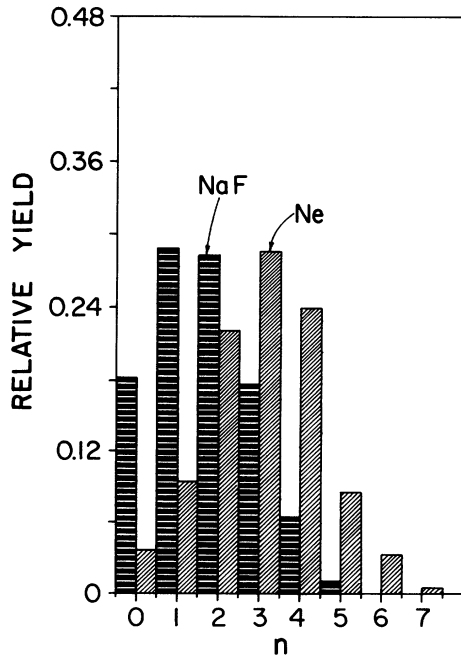


FIG. 4. Comparison of the satellite intensities for NaF (corrected for fluorescence yield) with the L-vacancy distribution determined for neon.

The probabilities f_K and f_x are also related via the fluorescence yield

$$f_x(n,j) = \omega(n,j) f_K(n,j)$$

defined in the usual way as

$$\omega(n,j) = \frac{\lambda_x(n,j)}{\lambda_x(n,j) + \lambda_A(n,j)}. \quad (2)$$

Since the individual multiplet states are not resolved in the x-ray spectra, the decay probability must be averaged over all states contributing to the KL^n x-ray group

$$f_i(n) = \sum_j p(n,j) f_i(n,j), \quad (3)$$

where $p(n,j)$ is the population probability for state j . If the states are populated statistically, the population probabilities are given by

$$p(n,j) = \frac{\{2L(j)+1\}\{2S(j)+1\}}{\sum_j \{2L(j)+1\}\{2S(j)+1\}}.$$

The fluorescence yield, averaged over all the multiplet states such that $f_x(n) = \omega(n) f_K(n)$, is no longer independent of λ_t ;

$$\omega(n) = \frac{f_x(n)}{f_K(n)} = \frac{\sum_j p(n,j) \left\{ \frac{\lambda_x(n,j)}{\lambda_T(n,j)} \right\}}{\sum_j p(n,j) \left\{ \frac{\lambda_K(n,j)}{\lambda_T(n,j)} \right\}}. \quad (4)$$

Therefore, using average theoretical fluorescence yields such as those given by Bhalla⁸ and by Chen and Crasemann⁹ to analyze x-ray spectra for cases involving electron transfer is clearly incorrect since these numbers are calculated using the relationship

$$\omega'(n) = \sum_j p(n,j) \left\{ \frac{\lambda_x(n,j)}{\lambda_K(n,j)} \right\}. \quad (5)$$

It is instructive to consider the limiting cases where (a) $\lambda_t = 0$ and (b) $\lambda_t \gg \lambda_K$. In the first case, Eq. (5) is applicable. In the second case, under the added assumption that λ_t is independent of j , the average fluorescence yield, as defined by Eq. (4), reduces to

$$\omega''(n) = \frac{\sum_j p(n,j) \lambda_x(n,j)}{\sum_j p(n,j) \lambda_K(n,j)} = \frac{\lambda_x(n)}{\lambda_K(n)}. \quad (6)$$

Fluorescence yields based on these two limiting cases [i.e., $\lambda_t = 0$; Eq. (5) and $\lambda_t \gg \lambda_K$; Eq. (6)] are compared in Table II. The values of $\lambda_x(n,j)$ and $\lambda_A(n,j)$ were taken from the calculations of Chen and Crasemann⁹ for Ne. It is evident from Table II

TABLE II. Limiting values of $K\alpha$ satellite fluorescence yields for Ne. (The rate constants are in units of 10^{-4} a.u.)

n	$\lambda_x(n)^a$	$\lambda_A(n)^a$	$\omega'(n)$	$\omega''(n)$
0	1.49	92.1	0.0159	0.0159
1	1.45	83.0	0.0175	0.0172
2	1.37	68.9	0.0199	0.0195
3	1.25	53.6	0.0248	0.0228
4	1.12	37.2	0.0390	0.0293
5	0.93	21.3	0.0862	0.0417
6	0.67	7.81	0.229	0.0790

^aFrom Ref. 9.

that the limiting fluorescence yields are not significantly different for $n < 3$, but that for $n = 5$ and 6, the values of ω' are more than twice those for ω'' .

The probability that a KL^n state will decay to a KL^m state by electron transfer and then decay by x-ray emission is

$$g(n, m) = f_x(m) f_t(m+1) \cdots f_t(n). \quad (7)$$

Hence, if the number of atoms left in KL^n states as a result of ion-atom collisions is $N^0(n)$, then the number of x rays observed in the KL^m group will be

$$N_x(m) = \sum_{n=m}^8 g(n, m) N^0(n). \quad (8)$$

The procedure used in the present analysis involved the computation of the x-ray intensities expected for each KL^n group [using Eq. (8)] under the assumption that the rate constant for electron transfer to the L shell is independent of j and that

$$\lambda_t(n) = n\lambda_t.$$

The values of $N^0(n)$ were derived from the neon measurements, as will be discussed below, and each f_t used in the calculation of $g(n, m)$ [Eq. (7)] was averaged over all the appropriate multiplet states using the theoretical x-ray and Auger rates of Chen and Crasemann.⁹ A statistical population of states was assumed. By repeating these calculations for different assumed values of λ_t until the calculated x-ray distribution matched the experimental one, the best estimate of λ_t was obtained.

In the analysis of the Ne spectrum to deduce the primary vacancy distribution, the satellite x-ray relative intensities were converted to relative vacancy yields using theoretical fluorescence yields, and corrections were applied to account for the partial quenching of metastable states in subsequent Ne-Ne collisions. The details of this analysis will be given elsewhere.⁵ The resulting p_L value was then corrected for projectile energy loss in the gas-cell window

($\Delta E = 5$ MeV) using the linear dependence of p_L on v/q taken from the recent work of Beyer *et al.*¹⁰ The corrected result for 22-MeV C ions on Ne was $p_L = 0.32 \pm 0.02$. This value agrees well with the results of Kauffman *et al.*,¹¹ as is shown in Ref. 5. Finally, the p_L value for the primary vacancy distribution in F^- was deduced from this result by taking into account the target- Z dependence. Measurements of the satellite intensities induced by 5.5-MeV He^+ in Na^+ (NaF) and Ne indicated that p_L increases by about 15% in going down in Z from one element to the next. (The influence of electron transfer on the low states of ionization in Na produced by 5.5-MeV He^+ is negligible.) Based upon the above observation the p_L value for the primary vacancy distribution generated by 22-MeV C ions on F^- was taken to be 0.37 ± 0.03 .

Application of the analysis procedure described above yielded values for the ratio $\lambda_t/\lambda_K(1)$ of 0.33, 0.37, and 0.38 for LiF, NaF, and MgF_2 , respectively. The calculated x-ray distributions were all in excellent agreement with the measured distributions. Table III lists values of the electron-transfer probabilities f_t and average fluorescence yields calculated for $\lambda_t/\lambda_K(1) = 0.33$. It is interesting to note that for the higher KL^n groups, the electron-transfer probability becomes much larger than the K -vacancy decay probability, which is $1 - f_t$, and the fluorescence yields approach the ω'' limit (see Table II).

The analysis of the NaF spectrum was repeated using the rather unrealistic assumption that λ_t is independent of both j and n . In this case the resulting ratio of $\lambda_t/\lambda_K(1)$ was 1.0 and satisfactory agreement between the calculated and measured x-ray distributions could not be achieved, as may be seen from Fig. 5. It may be further noted that the predicted intensity distribution is not binomial.

B. Resonant electron transfer

An analysis of the relative intensities of the KL^0 , KL^1 , and KL^2 x-ray groups excited by 5.5-MeV He^+ bombardment of the alkali-metal and alkaline-

TABLE III. Values of the electron-transfer probabilities and average fluorescence yields calculated with $\lambda_t/\lambda_K(1) = 0.33$.

n	f_t	ω
0	0	0.0159
1	0.251	0.0174
2	0.447	0.0197
3	0.612	0.0235
4	0.753	0.0304
5	0.871	0.0442
6	0.955	0.0850

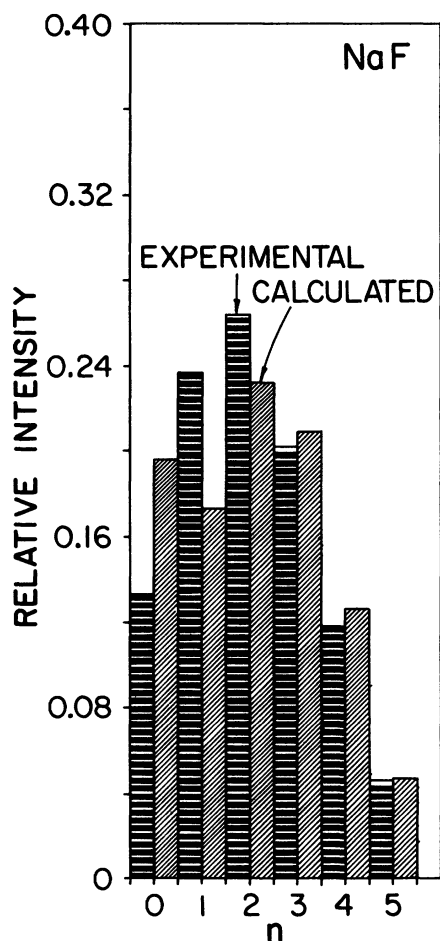


FIG. 5. Comparison of the experimental satellite intensity distribution for NaF with that calculated under the assumption that the rate constant for L -vacancy filling (λ_i) is independent of the number of L vacancies.

earth fluoride series was carried out previously.⁴ In that work, it was found that the KL^1 peak intensities for KF and SrF₂ were anomalously low compared to the other members of the two series. The proposed explanation for this behavior was a resonant electron transfer (RET) from the outer np levels of the neighboring metal ions to the $2p$ levels of fluorine ions having the vacancy configuration $1s^{-1}2p^{-1}$. The condition under which this resonance will occur is when the energy required for the electron (or vacancy) transfer is essentially zero.

The effect of RET on the KL^1 peaks of KF, SrF₂, and BaF₂ is visible in the spectra excited by 22-MeV carbon ions shown in Fig. 2. As noted previously, RET causes a transfer of intensity from the KL^1 peak to the KL^0 peak. In addition to verifying the He-ion results, the present spectra provide an oppor-

tunity to investigate the possible occurrence of RET in association with higher-order satellite peaks. A particularly interesting spectrum in this regard is that for CaF₂ (see Fig. 2). In this spectrum, the KL^2 peak intensity appears to be considerably depressed and the KL^0 and KL^1 peaks enhanced compared to the spectra for LiF, NaF, and MgF₂.

The resonance condition for a double- L -vacancy state is not as obvious as it is for a single- L -vacancy state. In terms of a molecular model in which the metal-ion np electrons and the fluorine-ion $2p$ electrons all contribute to the formation of a molecular orbital, it is clear that both vacancies must be shared. Thus, one is led to predict three possible outcomes of the radiative decay of the K vacancy in such a situation. Namely, at the time the fluorine K -vacancy decays either (a) both outer vacancies reside on the fluorine ion, in which case a KL^2 x ray is emitted, or (b) one outer vacancy resides on the fluorine ion and one resides on the metal ion, in which case a KL^1 x ray is emitted or (c) both outer vacancies reside on the metal ion, in which case a KL^0 x ray is emitted. The effect of double-vacancy RET on the observed spectrum would then be to transfer intensity from the KL^2 peak to the KL^1 and KL^0 peaks.

Since the molecular model requires a stationary state whose total energy is independent of the location of the vacancies, it does not appear that the resonance condition can be obtained from the simple electrostatic potential considerations that were used in the single-vacancy case.⁴ Nevertheless, it is worth noting that a double-vacancy resonance condition deduced by analogy with the single-vacancy resonance condition does in fact predict a resonance for CaF₂. It was shown previously that the resonance condition for the single- L -vacancy case (KL^1) is given by (neglecting polarization energies)

$$\Delta E(KL^1) = E_M^{FI}(np) - E_F^{FI}(2p; 1s^{-1}) + E^\alpha + e^2/R = 0, \quad (9)$$

where $E_M^{FI}(np)$ is the free-ion binding energy of an np electron in the metal, $E_F^{FI}(2p; 1s^{-1})$ is the free-ion binding energy of a $2p$ electron in a fluorine ion having a $1s$ vacancy, E^α is the sum of metal and fluorine-ion Madelung energies, and e^2/R is the extra Coulomb energy required to remove a metal-ion np electron due to the $1s$ vacancy in the neighboring fluorine ion. The above formula states that the energy required to produce an np vacancy in the metal ion must equal the energy required to produce a $2p$ vacancy in a fluorine atom already having a $1s$ vacancy. The analogous requirement applied to the double-vacancy case is that the energy needed to produce a second np vacancy in the metal ion must

equal the energy needed to produce a second $2p$ vacancy in a fluorine ion already having a $1s$ and a $2p$ vacancy:

$$\Delta E(KL^2) = E_M^{\text{FI}}(np; np^{-1}) - E_F^{\text{FI}}(2p; 1s^{-1}2p^{-1}) + E^\alpha + e^2/R = 0, \quad (10)$$

where $E_M^{\text{FI}}(np; np^{-1})$ is the free-ion binding energy of an np electron in a metal ion having an np vacancy and $E_F^{\text{FI}}(2p; 1s^{-1}2p^{-1})$ is the free-ion binding energy of a $2p$ electron in a fluorine ion having a $1s$ and a $2p$ vacancy.

The values obtained for $\Delta E(KL^2)$ using Eq. (10) are listed in Table IV. In the calculations, free-ion binding energies for the metal ions were taken from the compilation of Moore.¹² The Madelung energies and Coulomb energies were the same as those used in Ref. 4. A value of 41.6 eV was used for the fluorine-ion $2p$ binding energy as calculated using the Hartree-Fock program of Fischer.¹³ It can be seen in Table IV that only for CaF_2 does this resonance condition come close to being satisfied.

C. Enhancement of KL^0

As may be seen from Fig. 2, many of the spectra have KL^0 peaks that are much more intense than would be expected from a binomial fit to the higher-order satellite intensities. Even the KL^0 intensities for LiF , NaF , and MgF_2 are somewhat enhanced (see Fig. 3). In the cases of KF , SrF_2 , CaF_2 , and BaF_2 , the enhancement is partly due to RET. However, even taking RET into account, there appears to be an additional component present.

Possible KL^0 enhancement mechanisms include (a) K -shell photoionization by satellite and hypersatellite x rays above the fluorine absorption edge, and (b) K -shell ionization by secondary electrons scattered by the projectile. We have ruled out (a) because the enhancement is not thickness dependent. The likelihood that mechanism (b) is responsible for the enhancement is strengthened by the fact that the maximum energy transfer from a 22-MeV carbon

ion to a free electron (~ 4 keV) is well above the K -shell binding energy of fluorine.

The enhancement contributions were deduced from the measured spectra by making comparisons with theoretical intensity distributions calculated as described in Sec. IV A. It was assumed that the calculated intensities of the KL^0 and KL^1 peaks [$Y(0)$ and $Y(1)$, respectively] could be expressed in terms of their measured intensities [$N(0)$ and $N(1)$], a KL^0 intensity enhancement component E , and a transferred intensity component T due to RET, such that

$$Y(0) = N(0) - E - T,$$

$$Y(1) = N(1) - fE + T.$$

Because of shakeoff, the KL^1 peak is also enhanced by the amount fE where f is the KL^1 to KL^0 ratio observed in photoionization. For fluorine, f is approximately 0.4.¹⁴ The determination of E was accomplished by a trial and error procedure in which initial values of E and T were guessed and used to correct the measured relative intensities. The corrected relative intensities were then renormalized and the p_L value of the new distribution computed. Next, the corrected intensity distribution was compared to a theoretical distribution having the same p_L value, and new values of E and T guessed. The process was repeated until the best match between the corrected experimental distribution and a theoretical distribution was obtained. A comparison of the RET and enhancement corrected intensity distribution for SrF_2 with (a) the original experimental intensity distribution, and with (b) the theoretical distribution resulting from the application of the above procedure is shown in Fig. 6. The values of $\lambda_t/\lambda_K(1)$ obtained using the corrected intensity distributions are listed in Table V for each of the compounds.

To test the plausibility of secondary-electron ionization being the source of the KL^0 enhancement, the enhancement factors $E/N(0)$ were compared with stopping-power data.¹⁵ It is reasonable to assume that the number of secondary electrons produced is proportional to the energy loss of the projectile. To compare with the x-ray intensity resulting from projectile ionization, an arbitrary thickness of each target containing an equal number of fluorine atoms per cm^2 is taken. Then, assuming that the effective range of the secondary electrons in units of atoms per cm^2 is essentially the same for all the targets, the total energy loss should be proportional to the x-ray intensity resulting from secondary-electron ionization. Figure 7 shows a graph of relative enhancement versus relative energy loss. In order to compare the results for the two sets of compounds on

TABLE IV. Values of $\Delta E(KL^2)$ and of the metal-ion binding energies used in the calculations (in eV).

Compound	$E_M^{\text{FI}}(np; np^{-1})^a$	$\Delta E(KL^2)$
NaF	71.7	14.6
KF	46	-9.0
RbF	40	-14.4
CsF	34.6	-17.7
MgF_2	109.3	40.1
CaF_2	67	0.8
SrF_2	57	-7.8

^aFrom Ref. 11.

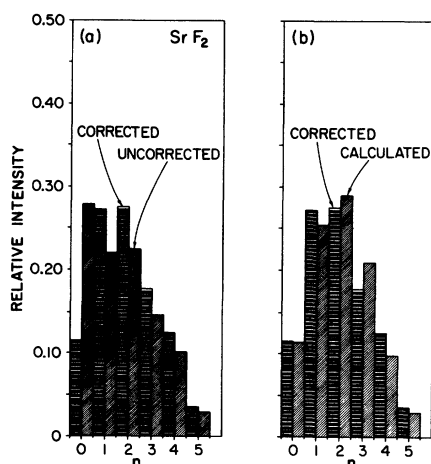


FIG. 6. Comparison of the RET and enhancement corrected intensity distribution for SrF_2 with (a) the original experimental distribution, and (b) with the calculated distribution.

the same scale, the enhancement factor $E/N(0)$ for the alkaline-earth fluorides has been multiplied by $\frac{3}{4}$ to account for the fact that $\frac{2}{3}$ of the atoms in these compounds are fluorine atoms whereas in the alkali-metal compounds only $\frac{1}{2}$ of the atoms are fluorine. A definite correlation does appear to exist, and hence it is concluded that secondary-electron ionization is most likely the cause of the observed enhancement.

The enhancement factor for CaF_2 was not included in Fig. 7 since if KL^2 RET transfers intensity from KL^2 to KL^1 and KL^0 , it is not possible to extract a unique value of E using the method described above. On the other hand, if the CaF_2 spectrum is analyzed without taking KL^2 RET into account, the enhancement factor which results is roughly 72%

TABLE V. Values of $\lambda_t/\lambda_K(1)$ obtained using the x-ray satellite relative intensities corrected for RET and secondary-electron enhancement.

Compound	$\lambda_t/\lambda_K(1)$
LiF	0.306
NaF	0.280
KF	0.261
RbF	0.142
MgF_2	0.332
CaF_2	0.423 ^a
SrF_2	0.392
BaF_2	0.197

^aUncorrected for KL^2 RET.

too large compared to the value predicted by the dashed line in Fig. 7. This fact provides additional support for the postulated presence of KL^2 RET in CaF_2 .

V. CONCLUSION

The fluorine $K\alpha$ satellite spectra of the alkali-metal and alkaline-earth fluorides, excited by 22-MeV carbon ions, have been examined in detail. The spectra for LiF, NaF, and MgF_2 were found to be well represented by binomial distributions, as has been commonly observed to be characteristic of such spectra for higher- Z elements. A comparison of the intensity distributions of the above compounds with the intensity distribution exhibited by the isoelectronic, monatomic gas neon revealed that L -vacancy filling prior to K x-ray emission is a highly probable occurrence in these solids. An analysis based on the assumption that the rate constant for L -vacancy transfer scales directly with the number of L vacancies yielded good agreement between the measured and calculated intensity distributions and indicated that the rate constant for single- L -vacancy filling (KL^1 to KL^0) ranges from about 20% to 40% that for K -vacancy decay in the alkali-metal and alkaline-earth fluorides.

Large deviations from binomial distributions were observed in the spectra for the other compounds. In the cases of KF, SrF_2 , and BaF_2 , these deviations are caused by RET, which depresses the intensity of KL^1 and enhances the intensity of KL^0 . The spec-

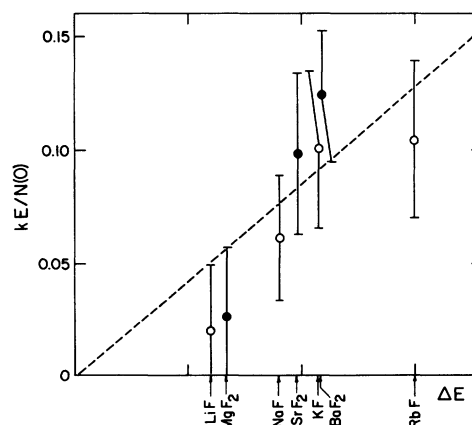


FIG. 7. KL^0 enhancement factor plotted vs the relative energy loss of the projectile. Dashed line has been fit to the data with the requirement that it have a zero intercept. The factor R is 1 for the alkali-metal fluorides and 0.75 for the alkaline-earth fluorides as explained in the text.

trum for CaF_2 exhibited enhanced KL^0 and KL^1 peaks, suggesting the possibility that RET occurs for the double- L -vacancy KL^2 states in this compound.

Another component which contributes to the enhancement of the KL^0 peak was attributed to secondary-electron-induced ionization. By taking L -vacancy transfer, resonant electron transfer, and secondary-electron ionization into account, a fairly complete understanding of all the spectra was achieved.

ACKNOWLEDGMENTS

We thank David Oldham, Timothy Ritter, and Bryan Bandong for help with the experiments. Discussions of resonant electron transfer with R. A. Kenefick are gratefully acknowledged. This work was supported by the U.S. Department of Energy, Office of Basic Energy Sciences, Division of Chemical Sciences, the Robert A. Welch Foundation, and the Texas A&M University Center for Energy and Mineral Resources.

¹R. L. Watson, A. K. Leeper, B. I. Sonobe, T. Chiao, and F. E. Jenson, *Phys. Rev. A* **15**, 914 (1977).

²J. A. Demarest and R. L. Watson, *Phys. Rev. A* **17**, 1302 (1978).

³M. Uda, H. Endo, K. Maeda, Y. Awaya, M. Kobayashi, Y. Sasa, H. Kumagai, and T. Tonuma, *Phys. Rev. Lett.* **42**, 1257 (1979).

⁴O. Benka, R. L. Watson, and R. A. Kenefick, *Phys. Rev. Lett.* **47**, 1202 (1981).

⁵R. L. Watson, O. Benka, K. Parthasaradhi, R. J. Maurer, and J. M. Sanders, *J. Phys. B* (in press).

⁶R. T. Poole, J. Leisegang, R. C. G. Leckey, and J. G. Jenkin, *Chem. Phys. Lett.* **23**, 194 (1973); R. T. Poole, J. Szajman, R. C. G. Leckey, J. G. Jenkin, and J. Leisegang, *Phys. Rev. B* **12**, 5872 (1975).

⁷R. Mann, F. Folkmann, and H. F. Beyer, *J. Phys. B*

Phys. **11**, L363 (1981).

⁸C. P. Bhalla, *Phys. Rev. A* **12**, 122 (1975).

⁹M. H. Chen and B. Crasemann, *Phys. Rev. A* **12**, 959 (1975).

¹⁰H. F. Beyer, R. Mann, and F. Folkman, *Nucl. Instrum. Methods* (in press).

¹¹R. L. Kauffman, C. W. Woods, K. A. Jamison, and P. Richard, *Phys. Rev. A* **11**, 872 (1975).

¹²C. E. Moore, *Atomic Energy Levels as Derived from Analyses of Optical Spectra*, NBS Circular No. 467 (U.S. GPO, Washington, D.C., 1949–1958), Vols. I–III.

¹³C. F. Fischer, *Comput. Phys. Commun.* **1**, 151 (1969).

¹⁴T. Aberg, *Phys. Lett.* **26A**, 515 (1968).

¹⁵L. C. Northcliffe and R. F. Schilling, *Nucl. Data Tables A* **7**, 233 (1970).